In situ imaging of mitochondrial translation shows weak correlation with nucleoid DNA intensity and no suppression during mitosis

Christopher Estell*, Emmanouela Stamatidou**, Sarah El-Messeiry***,**** and Andrew Hamilton***#

* Institute of Cancer Science, Glasgow University. UK. c.estell.1@ research.gla.ac.uk

** Evosmos, Thessaloniki, Greece. emmanouela93@gmail.com

*** School of Medicine, Dentistry and Nursing, Glasgow University. UK. s.ibrahim-elmesseiry.1@research.gla.ac.uk; andrew.hamilton@glasgow.ac.uk

**** Department of Genetics, Faculty of Agriculture, Alexandria University, Egypt

Corresponding author.

Key words: mitochondria translation labelling fluorescence click

Abstract. Although mitochondrial translation produces only 13 proteins, we show here how this can be labelled and detected *in situ* by fluorescence microscopy with a simple, rapid and inexpensive procedure using non-canonical amino acid labelling and click chemistry. This allows visualisation of the translational output in different mitochondria within a cell, their position within that cell and a comparison of mitochondrial translation between cells. Most highly translationally active mitochondria were closest to the nucleus but were also found at the distal end of long cellular projections. There were substantial differences in translation between adjacent mitochondria and this did not readily correlate with apparent Mt-genome content. Mitochondrial translation was unchanged during mitosis when cytoplasmic translation was suppressed. This method will serve both fundamental cell biology and clinically orientated studies in which mitochondrial function is a key parameter.

Introduction

Mitochondria are unique among animal organelles in that they possess their own genome. This expresses only 13 (Gustafsson *et al.*, 2016) proteins in contrast to over one thousand mitochondrial (Mt) proteins encoded by the nuclear genome (Pagliarini *et al.*, 2008). Despite their relatively small number, mitochondrion-encoded proteins are essential components of the oxidative phosphorylation pathway and Mt-genome mutations are strongly linked with aging and other degenerative diseases (Park and Larsson, 2011). The number of mitochondria per cell is in the order of several hundred but this changes continuously due to fission and fusion of these organelles (Westermann, 2010). Mt-DNA is packaged in structures called nucleoids which usually contain 1 or 2 copies of the Mt genome, however higher copy number nucleoids exist (Kukat et al., 2011, Bogenhagen, 2012, Gustafsson et al., 2016) and, again due to fission/fusion, the exact number of nucleoids per organelle must vary continuously. Gene amplification is a common mechanism for increasing expression - plasmids and oncogenes being obvious examples - and it is reasonable to propose that increased Mt-DNA content per nucleoid or per organelle would result in increased protein synthesis. However, this has not been tested because no method exists to examine total Mt-genome and *de novo* expression simultaneously *in situ*. Mt-genome polymorphisms (heteroplasmy) is also common in mammalian cells (Larsson, 2010, He *et al.*, 2010) partly due to the much higher mutation rate of Mt-DNA compared to nuclear DNA (Taylor *et al.*) but again it is not known how such sequence variation affects overall genome expression. Heterogeneity of Mt-membrane potential and some Mt-enzymes' activities, have been observed and associated with disease (Wikstrom *et al.*, 2009) in a similar way to genetic polymorphism. However, the extent to which such physiological heterogeneity arises from Mt-genetic variability is again unknown partly due to the paucity of methods for imaging global mitochondrial gene expression.

Methods to image protein expression within mitochondria are limited to traditional immunofluorescence analyses of individual proteins. These show only the steady state level of that protein studied and do not reveal any dynamic changes or reveal rates of overall translation. Global synthesis of new Mt-encoded proteins has been studied either using radioactively (^{35}S) labelled methionine (met) (Sasarman and Shoubridge, 2012, Gao et al., 2016), or non-canonical amino acid analogues of Met (Zhang *et al.*, 2014). Both procedures used either PAGE or MS analyses of protein extracts and were therefore blind to inter-mitochondrion variation or the spatial distribution of translationally active mitochondria within the cells. Non-canonical amino acid labelling can also be used for *in situ* imaging of total cytoplasmic protein synthesis because the incorporated amino acid analogues can be coupled to fluorescent reporter molecules after labelling via chemo-selective, bio-orthogonal click reactions. This allowed detection only of proteins synthesised during the labelling period by fluorescence microscopy i.e. without interference from pre-existing proteins (Dieterich *et al.*, 2006, Beatty, 2006, Beatty, 2011). However, the sensitivity of these methods apparently did not extend beyond detection of total cytoplasmic protein

synthesis which, of course, constitutes the vast majority of a cell's translational output. In these reports, confirmation that labelling was the result of translation was demonstrated by the absence of detectable labelling in the presence of cycloheximide (CHI), a potent inhibitor of cytoplasmic translation. Mt-translation, which is insensitive to CHI, was not detected in these experiments although it is known to incorporate these non-canonical amino acids (Zhang *et al.*, 2014). It is likely that since Mt-translation produces only 13 proteins, labelling of these was below the threshold of detection available with the procedures employed. In this report we describe how labelling cells with a non-canonical amino acid and then "click" reaction with a fluorescent azide can in fact be used to observe global Mt-translation *in situ* by epi-fluorescence microscopy. We show how the background fluorescence, which would otherwise obstruct detection of Mt-translation, can be eliminated by a simple adjustment to the cell fixation procedure. The method reveals the spatial heterogeneity of Mt-translational output within a cell and it's consistency through mitosis. These demonstrate the utility of our method for both fundamental and clinically-orientated studies of Mt-gene expression.

Results

Cell permeabilising before cell fixation greatly reduces background fluorescence after HPG labelling

In the first report of *in situ* protein synthesis imaging using the "clickable" Met analogue, homopropargylglycine (HPG), genuine incorporation by cytoplasmic translation in mouse embryonic fibroblasts was confirmed by elimination of detectable signal by CHI (Beatty, 2006). Following a similar labelling and fixation procedure we observed similar HPG incorporation in mouse C2C12 cells (Figure 1Ai) that was also strongly suppressed by CHI (Figure 1Aii). Suppression of cytoplasmic translation by CHI should have revealed the underlying Mt-translation. However, our attempts to observe this by extending the fluorescence exposure time of HPG+CHI treated cells were confounded by excessive background fluorescence (Figure 1Bii). This background signal was undiminished by high concentrations of puromycin (Figure 1Biii) which should inhibit all HPG incorporation by protein synthesis but was absent from cells not given HPG (Figure 1Bi) suggesting it originated from trapped HPG reacting with the fluorescent azide. We had followed the procedure of Beatty *et. al.* (2006) that employed a widely used formaldehyde-based cell fixation procedure followed by cell permeabilising with detergent. Therefore, we investigated whether briefly permeabilising the cells *before* fixation with digitonin, a detergent that has a minimal effect on mitochondria, would allow escape of free HPG and thus reduce background signal. This simple modification all but eliminated the background fluorescence leaving a fainter but clear punctate / rod-like pattern (compare Figure 1B-ii with 1C-ii) that was stronger and distinct from the trace fluorescence in no-HPG treated control cells (compare Figure 1C-ii and 1C-i).

CHI-resistant HPG labelling is qualitatively different to HPG without CHI

It was possible that the pattern observed in CHI-treated cells made permeable before fixation (Figure 1Cii) was simply due to incomplete inhibition of cytoplasmic translation by CHI i.e. a weak version of HPG-only. Therefore, we compared the pattern of total cytoplasmic translation and putative mitochondrial translation using the optimised permeabilisation and fixation procedure (Figure 2). Without CHI there was rapid synthesis and nuclear import of nucleolar proteins which made up a substantial proportion of the total new protein made. Also, new proteins were observed distributed throughout the cytoplasm (Fig 2Ai). In contrast, with CHI (Fig 2Bi), there was no nucleolar signal and the cytoplasmic pattern was punctate/rod-like rather than diffuse. Although long exposure times were necessary to detect this pattern the signal strength was still 20-200 fold higher than background fluorescence levels (Fig 2 Biii,iv). Essentially the same differential (HPG vs HPG+CHI) labelling pattern was observed in murine Eph4 and human MCF-7 cells (Supplementary Figures 1 and 2).

***In situ* CHI-resistant labelling with HPG is the result of mitochondrial protein synthesis**

If the HPG+CHI signal truly represented mitochondrial translation it should be resistant to other antibiotics that selectively inhibit cytoplasmic translation irrespective of their mechanism or the stage of translation they affect. Figure 3ii shows that Harringtonine, an elongation inhibitor like CHI, allowed HPG incorporation in the same pattern as with CHI (Figure 3i). Pactamycin, which inhibits cytoplasmic translation initiation, also generated this pattern indicating it was not due to HPG-labelled nascent proteins arrested on stalled polyribosomes (Figure 3iii). Puromycin, which inhibits both cytoplasmic and Mt-translation (but not amino acyl transferases)(Pestka, 1971), eliminated the signal, confirming it was due to genuine protein synthesis and not residual unincorporated HPG retained within the fixed cells or HPG-charged tRNA (Figure iv). Chloramphenicol (CAP), which specifically inhibits Mt-translation in eukaryotic cells (Sasarman and Shoubridge, 2012), combined with CHI also eliminated the signal (Figure 3v). Together, these results strongly suggested the CHI-resistant signal was from Mt-translation.

CHI resistant HPG labelling co-localises with Mt-expressed protein, Mt-12s rRNA and nucleoid DNA but shows unexpected heterogeneity

The total products of *de novo* Mt translation should co-localise in pattern near-perfectly with specific Mt proteins detected by immunofluorescence (IF). Figure 4 i-iii shows the HPC+CHI signal strongly co-localising (mean Pearson correlation coefficient = 0.9) with the Mt-encoded cytochrome oxidase 1 (MT-CO1) protein. There was some discrepancy in intensity (but not pattern) between MT-CO1 IF and HPG+CHI signal particularly at the distal end of the long cytoplasmic projections often observed with the C2C12 cell line which likely reflects the prolonged stability of MT-CO1 in mitochondria that have become translationally

less active. This illustrates the differences that can be observed when imaging steady state levels of proteins by IF versus more dynamic methods such as ours.

HPG+CHI signal also co-localised in pattern with both Mt 12s rRNA (Figure 4 iv-vi) detected by fluorescence *in situ* hybridisation (FISH) and nucleoid DNA detected by DAPI (Figure 4 vii-ix. Here the fine structure co-localisation was not as complete as with the IF, which is to be expected, as the translation products will distribute throughout the inner Mt-membrane whereas nucleoid DNA and rRNA are more highly localised within the Mt-matrix.

Close examination of Mt-translation versus either Mt 12s rRNA or nucleoid DNA often revealed a lack of correlation in intensity by eye: spots of higher DAPI intensity were often not adjacent to regions of higher translation activity. Conversely, the latter could often be found adjacent to weak or barely visible DAPI staining spots. This lack of correlation was more apparent in the MCF-7 cells (Figure 5A) which often contained several strongly DAPI staining spots along the mitochondrial network (as revealed by translation imaging; Figure 5A iv) which were clearly not sites of elevated translational activity. Signal intensity for HPG and DAPI were measured using ImageJ (materials and methods), plotted and a regression line calculated (Figure 5B). The low coefficient of determination ($R^2 = 0.3458$) supports the argument that there is not a simple, positive, linear relationship between nucleoid DNA amount and translational activity. Note that the DNA signal was not due to *mycoplasma* infection*:* these cell lines tested negative with a commercial *mycoplasma spp.* test kit. DAPI visualisation of *mycoplasma DNA* does not require the extended exposure times (Uphoff *et al.*, 1992) used here since their genomes are far larger than the Mt-genome. Furthermore, MT-CO1 co-localised with the punctate, cytoplasmic DAPI signal confirming the latter as mitochondrial nucleoid DNA (Supplemental Figure 3).

Mitochondrial translation is not suppressed during mitosis

In situ imaging of cultured cells by DAPI staining readily reveals any cells in mitosis. Translation on cytoplasmic ribosomes is generally thought to be strongly reduced at mitosis although early studies in fact showed the extent of suppression was highly dependent on the cell type studied (Prescott and Bender, 1962, Konrad, 1963). The majority of HPG incorporated by cells in the absence of inhibitors is from cytoplasmic ribosome translation and so suppression of proteins synthesis at mitosis can be easily observed combining DAPI staining and HPG incorporation. C2C12 cells showed little suppression of protein synthesis during mitosis whereas there was strong suppression in Eph4 cells and moderate suppression in MCF-7 cells (Figure 6A and Supplementary Figures 1 and 2). The same imaging but with CHI to reveal mitochondrial translation showed this was unaffected in any cell line (Figure 6B).

Discussion

We have developed a simple and rapid method of labelling *de novo* translation in mitochondria which allows it's *in situ* imaging by epifluorescence microscopy (Figure 1,2). The key step was permeabilising cells before fixation with a reagent (Digitonin) that leaves mitochondria intact but allows release of the unassimilated labelling amino acid that otherwise becomes fixed and fluorescently labelled obscuring any genuine signal from Mt protein synthesis. Mt labelling with the "click-able" amino acid analogue HPG was achieved by simultaneous inhibition of cytoplasmic translation by cycloheximide. The response of this CHI-resistant HPG labelling to other antibiotics was entirely consistent with incorporation on Mt ribosomes. Furthermore, we demonstrated that the *de novo* CHI-resistant HPG signal co-localised with Mt-specific markers i.e. MTCO1, MT-DNA and MT-12s-rRNA (Figure 4) detected by IF, DAPI staining and FISH respectively. These results also showed how our method can be easily combined with other commonly used methods in cell biology. It is also worth noting that our method does not require extensive (0.5-4 hours) pre-incubation of cells in Met-free medium used in other protein labelling protocols (Hodas *et al.*, 2012, Beatty, 2006, Dieterich *et al.*, 2006, Zhang *et al.*, 2014) mitigating concerns that artefactual translational programmes would be established before labelling treatments (Goodman *et al.*, 2012).

In the course of developing and testing the method we made two observations that exemplify the utility of our method and may serve as primers for further, more detailed, investigation. First was our observation that although spatial patterns of Mt rRNA and DNA matched the spatial pattern of translation closely, there was frequently little correlation of intensity. This was surprising as one might reasonably propose that Mt genome amplification would serve as a mechanism to boost Mt protein expression and that ribosome content might determine translational output. This appeared often not to be the case in the cancer cell line MCF-7 in particular, where we frequently observed a point cluster of multiple Mt-genomes well in numerical excess of other surrounding nucleoids/clusters but that had little associated translation. DAPI fluorescence of Mt-DNA correlates well with other methods for estimating Mt-DNA such as anti-DNA antibodies (Kukat et al., 2011) and so this is not likely due to inaccuracy of Mt-DNA quantification. It will be of interest to explore how silencing of the mitochondrial genome takes place and whether this is a response to other cellular failures or an instrumental stage in processes such as apoptosis.

In situ methods such as ours also readily allow observation of events during mitosis as this stage of the cell cycle is easily identified by DAPI staining. Cytoplasmic translation is generally thought to be suppressed at this stage (Prescott and Bender, 1962) and this was evident in Eph4 cells (Supp. Figure 1i) and to some extent in Mcf-10a cells (Supp. Figure 2i). Our method shows for the first time that Mt-translation during mitosis is not similarly suppressed (Supp. Figures 1v,vi and 2iii,iv). This raises questions as to how the cells would

balance the assembly of dual-genome-origin protein complexes during this phase of the cell cycle. Such observations illustrate the advantages of our *in situ* method for revealing unexpected results and generating new hypotheses to be tested.

The frequency and severity of Mt-disease makes it important to develop a range of tools with which to study Mt-biology (Park and Larsson, 2011). Our method will allow the investigation and comparison of the number, variation and cellular distribution of translationally active mitochondria in normal versus diseased cells yielding insight into disease aetiology and pathophysiology. Additionally, from a clinical perspective, some classes of important antimicrobial antibiotics cause side effects due to their inhibition of Mt-translation, which results from the prokaryotic ancestry of mitochondria (McKee *et al.*, 2006). A simple method of measuring Mt-translation would facilitate the screening and monitoring of side effects of new drugs in this class. Similarly, antiviral ribonucleoside analogues frequently have toxic side effects as a result of inhibition of Mt-RNA polymerase (Arnold *et al.*, 2012). Inhibition of Mt-transcription would be result in reduced Mt-translation, which again could be easily assessed with our method.

In conclusion, labelling with HPG in the presence of CHI is a rapid, simple and inexpensive method for the *in situ* detection of Mt-translation with which to investigate the spatio/temporal activity of mitochondria relative to: a) other cellular features, b) in response to internal and external signals and c) in relation to genetic differences both normal (e.g. genome content fluctuation) and pathological.

Materials and Methods.

Cell culture: C2C12 cells (mouse myoblast),Eph4 cells (mouse spontaneously immortalized mammary epithelium) and MCF-7 cells (human mammary carcinoma) were cultured in Dulbecco's modified Eagle's medium (Sigma) with 10 % foetal bovine serum, 4.5 $g.L^{-1}$ glucose, 110 $mg.L^{-1}$sodium pyruvate, 2 mM L-glutamine, 10 $\mu g.mL^{-1}$ streptomycin and 10 $units.mL^{-1}$penicillin. All cultured cells are routinely tested for *Mycoplasma spp.* Contamination using the Mycoalert™ kit (Lonza)

Translation labelling: For protein labelling and analysis, cells were grown on Lab-Tek™ II (Nunc), 8 well glass chamber slides until approximately 90 % confluent. Met-free medium (Sigma) was always supplemented with 2mM Glutamine and 0.0303 mg. $mg.ml^{-1}$ cysteine and was used with or without appropriate antibiotics. Immediately prior to labelling, slides were removed from the incubator and placed on a 37°C surface, existing medium was removed and replaced with pre-warmed met-free medium, this step lasted no more than one minute for any one well. We found no need for the extensive (at least 30 mins) pre-incubation and labelling incubation in Met-free conditions characteristic of previous studies and thought to be necessary to deplete cells of Met (Beatty, 2006, Hodas et al., 2012) Then, that medium was removed and replaced with pre-warmed met-free medium with or without appropriate antibiotics and with 1 mM homopropargylglycine (HPG) and the slide

placed back in the humidified CO_2 incubator for 10 minutes (or as long as the experiment required).

Cell fixation and click reaction: After that labelling period, slides were immediately placed on ice, medium was removed, washed with ice-cold Buffer A (10 mM HEPES/KOH pH 7.5; 10 mM NaCl; 5 mM $MgCl_2$; 300 mM sucrose). Immediate fixation was with Buffer A supplemented with 3.7 % formalin (1/10 dilution from 37 % stabilised formaldehyde solution) for 10 minutes followed by 20 minutes in PBS with 0.1% TritonX-100. For permeabilising before fixation, the cells were incubated on ice for 2 minutes in ice-cold buffer A supplemented with 0.015 % Digitonin. That permeabilising solution was then removed and replaced with Buffer A supplemented with 3.7 % formalin (1/10 dilution from 37 % stabilised formaldehyde solution) to fix the cells (30 minutes at room temperature). Cells were then washed several times in PBS. Click reactions were carried out in 100 mM Tris/HCl (pH8.8), 100 mM ascorbic acid, 1 mM $CuSO_4$ and 10 µM Alexa Fluor® 594-azide (Invitrogen) (or 10 µM Alexa Fluor® 488-azide, Jena Bioscience, Germany) for 15 minutes followed by further washing in PBS. DAPI was used at 0.2 $\mu g.ml^{-1}$ in PBS. In the case (Figure 4) where the click reaction followed RNA FISH, a different reaction formulation was used to minimise RNA degradation: 40 µM $CuSO_4$, 200 µM BTTAA ligand (Jena Bio, Germany), 10 µM sulpho-cy5 picolyl azide (Jena Bio, Germany), 5% DMSO, 1 mM ascorbic acid in PBS

***In situ* hybridisation:** Fixed cells on glass slides were incubated with 0.1µM Cy3 labelled (single, 5' terminal conjugate) oligonucleotide (TTACGCCGAAGATAATTAGTTTGGGTTAATCGTATGACCG) complementary to murine mitochondrial 12S rRNA in 2X SSC, 50% formamide, 10% dextran sulphate, 20 $\mu g.ml^{-1}$ tRNA (*E.coli*) at 60 °C for two minutes then at 40 °C for one hour followed by removed of unhybridised probe by washing in PBS at 40 °C.

Immunofluorescence: Fixed cells were incubated in PBS with 0.1% Trtion X-100, 2.5% Horse serum and 1/100 dilution anti-MT-CO1 antibody (Abcam, AB154477 (1D6E1A8), Alexa Fluor 488 labelled). Excess antibody was removed by washing in PBS with PBS.

Antibiotics and other reagents: Final concentrations of antibiotics used were cycloheximide (CHI; Sigma): 100 $\mu g.ml^{-1}$; Harringtonine (AbCam): 2 $\mu g.ml^{-1}$; puromycin (Sigma) 50 $\mu g.ml^{-1}$; pactamycin (Sigma) 1 µM; chloramphenicol (Sigma) 80 $\mu g.ml^{-1}$. All antibiotics were delivered to cells at the same time as HPG except chloramphenicol which was added to cells 20 minutes before (and during) incubation with HPG.

Microscopy and image analysis: All images were taken using an epi-fluorescence inverted microscope (Olympus X51, Japan) with a 40 X objective lens (Olympus Japan, aperture 0.6 with adjustable focus ring). Images were taken under total magnification of 400 X using a digital camera and acquired with the Cell P program at same exposure time for each fluorophore unless otherwise stated. Images were opened in Image J and those taken with the same filter and exposure time were set to identical pixel/intensity threshold settings. All

threshold alterations were linear using the brightness/contrast tool in ImageJ. Lower thresholds were raised only to blacken the space between cells, not within cells. Upper thresholds were lowered only make visible any weaker signal towards the edge of cells. Images were coloured using standard LUTs in Image J. Figures were assembled using Inkscape and without further intensity manipulation. Co-localisation analysis was carried out individually on 18 cells (entire cell outline) using Image J with the COL2 plugin to generate Pearson's correlation. Mean and standard deviation of these measurements was calculated with Excel. For measurement of nucleoid DNA intensity, distinct DAPI staining spots (i.e. not obviously part of cluster) were selected blindly (i.e. without regard to translation intensity). We excluded those close to the nucleus to minimise fluorescence spill-over from nuclear DNA. Once chosen, a circle was drawn around the visible local translation surrounding or adjacent to that punctate DAPI signal and designated a region of interest (ROI).

Fluorescence intensity was measured using Image J: cell areas were selected manually and integrated total fluorescence calculated with the measurement tool. Background signal was measured from 8 independent selections in each image and the mean fluorescence determined. Finally, the total corrected cellular fluorescence (TCCF) for each cell was calculated using the following equation = [integrated fluorescence (density) – (area of selected cell × mean fluorescence of background readings)]. Linear regression and calculation of R^2 were performed using Microsoft Excel.

PAGE analysis of proteins: C2C12 cells were grown in standard TC flasks and labelled with HPG with or without inhibitors the same way as for cells grown on microscope slides (above). Protein was extracted by incubation of washed monolayer cells for 4 minutes in ice cold buffer 10 mM HEPES/KOH (pH 7.5); 10 mM NaCl; 300 mM sucrose; 5 mM $MgCl_2$; 1 % (v/v) Triton X100; 0.5 % (w/v) deoxycholate; 1 % (v/v) proteinase inhibitor cocktail (Sigma-Aldrich), recovery of the solution and precipitation of proteins from this with acetone. Biotin was coupled to HGP labelled proteins by "Click" reaction with PEG3-biotin-azide (Jena Bioscience, Germany) using the Click Chemistry Protein Reaction Buffer Kit (Dundee Cell Products, UK) and then recovered according to manufacturer's instruction. After PAGE, proteins were detected by Coomassie staining or after transfer to nitrocellulose membrane, incubation with Streptavidin-HRP (ThermoFisher, UK) and then a chemiluminscence substrate. Light emitted was measured and recorded using the LAS3000 instrument (FUJI) with a cooled CCD recorder.

Acknowledgements

We are grateful to Dr Torsten Stein, Ms Sylvia Garza Manero and Dr Anuradha Tarafdar for many helpful discussions of this work and critical reading of the manuscript and to anonymous referees for constructive suggestions. This work was funded by the University of Glasgow. Ms El-Messeiry is supported by a Newton-Mosharafa scholarship funded by the Egyptian Ministry of Higher Education and British Council and the British Embassy in Egypt.

Competing Interests

No competing interests declared

Author Contributions

CE, ES and AH carried out experimental work, CE, SE-M and AH analysed data, AH conceived the work, CE and AH wrote the manuscript

Funding

CE is supported by registered charity Friends of the Paul O'Gorman.

References

ANDERSON, M. F. & SIMS, N. R. 2000. Improved recovery of highly enriched mitochondrial fractions from small brain tissue samples. *Brain Research Protocols,* 5**,** 95-101.

ARNOLD, J. J., SHARMA, S. D., FENG, J. Y., RAY, A. S., SMIDANSKY, E. D., KIREEVA, M. L., CHO, A., PERRY, J., VELA, J. E., PARK, Y., XU, Y., TIAN, Y., BABUSIS, D., BARAUSKUS, O., PETERSON, B. R., GNATT, A., KASHLEV, M., ZHONG, W. & CAMERON, C. E. 2012. Sensitivity of Mitochondrial Transcription and Resistance of RNA Polymerase II Dependent Nuclear Transcription to Antiviral Ribonucleosides. *PLoS Pathog,* 8**,** e1003030.

BEATTY, K. E. 2011. Chemical strategies for tagging and imaging the proteome. *Molecular BioSystems,* 7**,** 2360-2367.

BEATTY, K. E., LIU, J.C., XIE, F., DIETERICH, D.C., SCHUMAN, E.M., WANG, Q. AND TIRRELL, D.A 2006. Fluorescence Visualization of Newly Synthesized Proteins in Mammalian Cells13. *Angewandte Chemie International Edition,* 45**,** 7364-7367.

BOGENHAGEN, D. F. 2012. Mitochondrial DNA nucleoid structure. *Biochimica et Biophysica Acta (BBA) - Gene Regulatory Mechanisms,* 1819**,** 914-920.

DIETERICH, D. C., LINK, A. J., GRAUMANN, J., TIRRELL, D. A. & SCHUMAN, E. M. 2006. Selective identification of newly synthesized proteins in mammalian cells using bioorthogonal noncanonical amino acid tagging (BONCAT). *Proceedings of the National Academy of Sciences,* 103**,** 9482-9487.

GAO, Y., BAI, X., ZHANG, D., HAN, C., YUAN, J., LIU, W., CAO, X., CHEN, Z., SHANGGUAN, F., ZHU, Z., GAO, F. & QIN, Y. 2016. Mammalian elongation factor 4 regulates mitochondrial translation essential for spermatogenesis. *Nat Struct Mol Biol,* 23**,** 441-449.

GOODMAN, C. A., PIERRE, P. & HORNBERGER, T. A. 2012. Imaging of protein synthesis with puromycin. *Proceedings of the National Academy of Sciences,* 109**,** E989.

GUSTAFSSON, C. M., FALKENBERG, M. & LARSSON, N.-G. 2016. Maintenance and Expression of Mammalian Mitochondrial DNA. *Annual Review of Biochemistry,* 85**,** 133-160.

HE, Y., WU, J., DRESSMAN, D. C., IACOBUZIO-DONAHUE, C., MARKOWITZ, S. D., VELCULESCU, V. E., DIAZ JR, L. A., KINZLER, K. W., VOGELSTEIN, B. & PAPADOPOULOS, N. 2010. Heteroplasmic mitochondrial DNA mutations in normal and tumour cells. *Nature,* 464**,** 610-614.

HODAS, J. J. L., NEHRING, A., HÖCHE, N., SWEREDOSKI, M. J., PIELOT, R., HESS, S., TIRRELL, D. A., DIETERICH, D. C. & SCHUMAN, E. M. 2012. Dopaminergic modulation of the hippocampal neuropil proteome identified by bioorthogonal noncanonical amino acid tagging (BONCAT). *PROTEOMICS,* 12**,** 2464-2476.

KONRAD, C. G. 1963. Protein synthesis and RNA synthesis during mitosis in animal cells. *The Journal of cell biology,* 19**,** 267-277.

KUKAT, C., WURM, C. A., SPÅHR, H., FALKENBERG, M., LARSSON, N.-G. & JAKOBS, S. 2011. Super-resolution microscopy reveals that mammalian mitochondrial nucleoids have a uniform size and frequently contain a single copy of mtDNA. *Proceedings of the National Academy of Sciences,* 108**,** 13534-13539.

LARSSON, N.-G. 2010. Somatic Mitochondrial DNA Mutations in Mammalian Aging. *Annual Review of Biochemistry,* 79**,** 683-706.

MCKEE, E. E., FERGUSON, M., BENTLEY, A. T. & MARKS, T. A. 2006. Inhibition of Mammalian Mitochondrial Protein Synthesis by Oxazolidinones. *Antimicrobial Agents and Chemotherapy,* 50**,** 2042-2049.

PAGLIARINI, D. J., CALVO, S. E., CHANG, B., SHETH, S. A., VAFAI, S. B., ONG, S.-E., WALFORD, G. A., SUGIANA, C., BONEH, A. & CHEN, W. K. 2008. A mitochondrial protein compendium elucidates complex I disease biology. *Cell,* 134**,** 112-123.

PARK, C. B. & LARSSON, N.-G. 2011. Mitochondrial DNA mutations in disease and aging. *The Journal of Cell Biology,* 193**,** 809-818.

PESTKA, S. 1971. Inhibitors of Ribosome Functions. *Annual Review of Microbiology,* 25**,** 487-562.

PRESCOTT, D. M. & BENDER, M. A. 1962. Synthesis of RNA and protein during mitosis in mammalian tissue culture cells. *Experimental Cell Research,* 26**,** 260-268.

SASARMAN, F. & SHOUBRIDGE, E. A. 2012. Radioactive Labeling of Mitochondrial Translation Products in Cultured Cells. *In:* WONG, P. D. C. L.-J. (ed.) *Mitochondrial Disorders: Biochemical and Molecular Analysis.* Totowa, NJ: Humana Press.

TAYLOR, R. W., BARRON, M. J., BORTHWICK, G. M., GOSPEL, A., CHINNERY, P. F., SAMUELS, D. C., TAYLOR, G. A., PLUSA, S. M., NEEDHAM, S. J., GREAVES, L. C., KIRKWOOD, T. B. L. & TURNBULL, D. M. Mitochondrial DNA mutations in human colonic crypt stem cells. *The Journal of Clinical Investigation,* 112**,** 1351-1360.

UPHOFF, C. C., GIGNAC, S. M. & DREXLER, H. G. 1992. Mycoplasma contamination in human leukemia cell lines. *Journal of Immunological Methods,* 149**,** 43-53.

WESTERMANN, B. 2010. Mitochondrial fusion and fission in cell life and death. *Nat Rev Mol Cell Biol,* 11**,** 872-884.

WIKSTROM, J. D., TWIG, G. & SHIRIHAI, O. S. 2009. What can mitochondrial heterogeneity tell us about mitochondrial dynamics and autophagy? *The international journal of biochemistry & cell biology,* 41**,** 1914-1927.

ZHANG, X., ZUO, X., YANG, B., LI, Z., XUE, Y., ZHOU, Y., HUANG, J., ZHAO, X., ZHOU, J., YAN, Y., ZHANG, H., GUO, P., SUN, H., GUO, L., ZHANG, Y. & FU, X.-D. 2014. MicroRNA Directly Enhances Mitochondrial Translation during Muscle Differentiation. *Cell,* 158**,** 607-619.

Figures

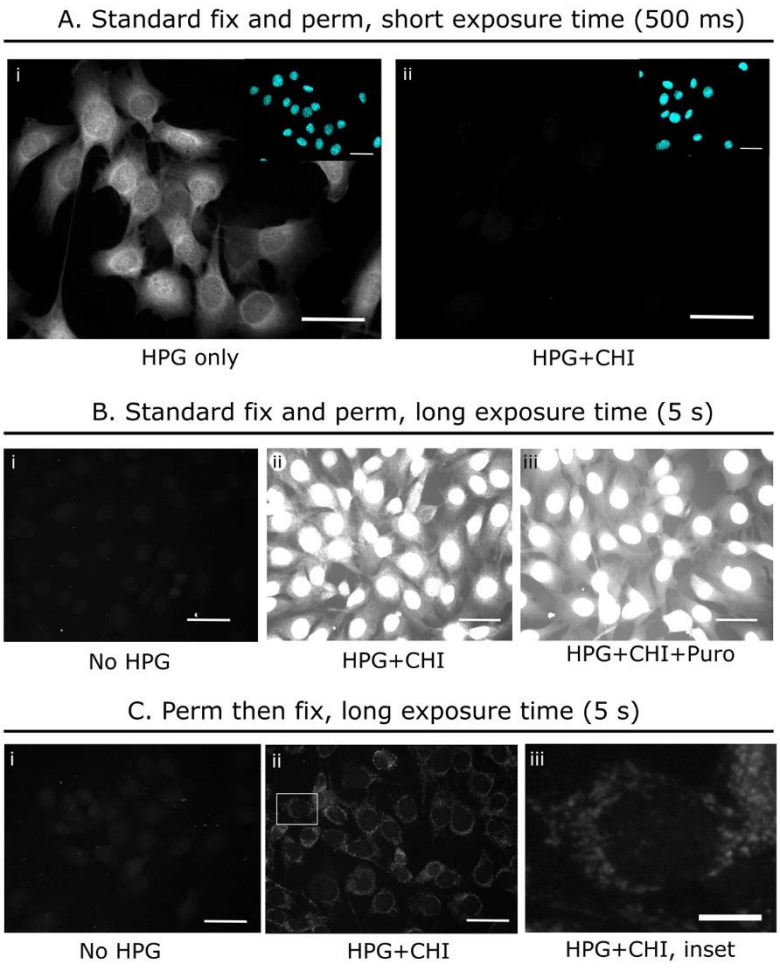

Figure 1: Background fluorescence observed from trapped HPG when using standard conditions can be removed by performing a pre-fix permbealisation. C2C12 cells were incubated for 10 minutes with HPG, with our without inhibitors (annotated) and proteins with incorporated HPG were labelled with a fluorescent azide *via* a "click" reaction, and imaged by epifluorescence microscopy. Standard conditions (A and B) employed a 10 minute formaldehyde fix followed by a 10 minute post-fix permbealisation using 0.1% TritonX-100. A: 500ms exposure time (DAPI stain shown in inset). B: 5 second exposure times were used for no-HPG (i), cycloheximide (CHI) (ii) and CHI and puromycin treated cells (iii). C. Optimised conditions employ a 2 minute pre-fix permbealisation using 0.015% Digitonin on ice followed by a 10 minute formaldehyde fix and 5 second exposure.Images within the same set (1A, 1B or 1C) have the same exposure times and are displayed with identical brightness and contrast settings. Scale bars: 50 µm, except inset C iii, 10 µm.

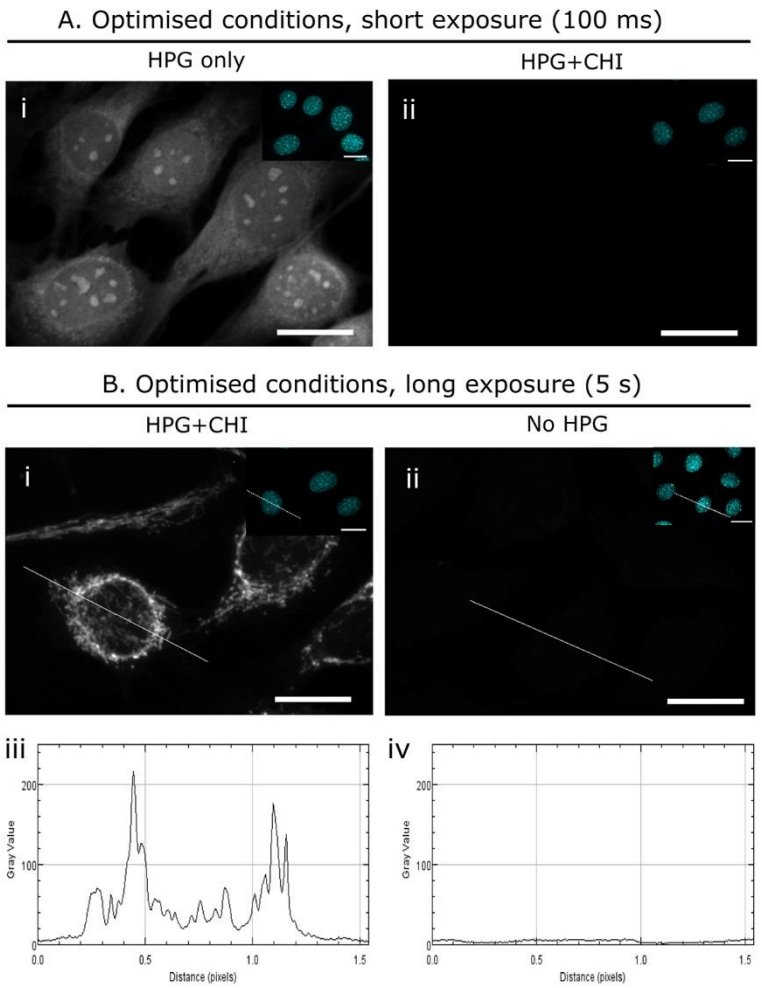

Figure 2: Qualitative assessment of protein synthesis in C2C12 cells with or without cycloheximide using optimised conditions. C2C12 cells were incubated for 10 minutes with HPG, with or without CHI, made permeable with 0.015% Digitonin for two minutes on ice, fixed for 10 minutes with formaldehyde. Proteins with incorporated HPG were labelled with a fluorescent azide *via* a "click" reaction, and imaged by epifluorescence microscopy with 100 ms (A) or 5 second (B) exposure times. No-HPG negative controls were exposed to the same click reaction with fluorophore to control for non-specific reactions or adsorbance. Relative fluorescence intensities along a line (in white) traversing a cells labelled with HPG+CHI or no HPG were calculated using the "plot profile" tool in ImageJ (Biii, iv). The DAPI staining of the same cells are shown in insets. Images with same exposure times are displayed with identical brightness and contrast settings. Scale bars: 20 µm.

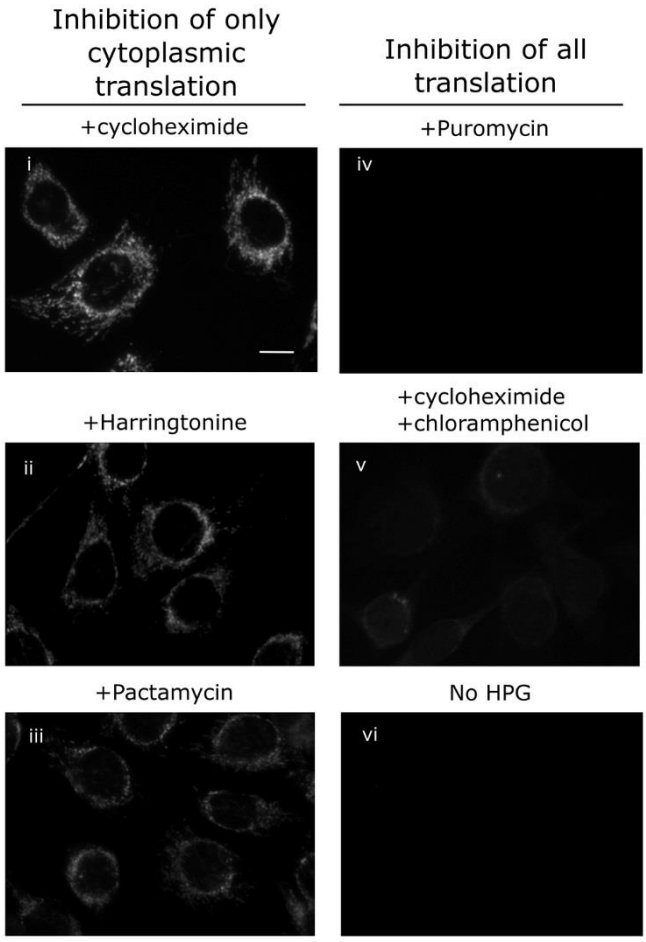

Figure 3: Fluorescent signal is not from HPG-charged tRNA, nascent proteins stalled on ribosomes during translation or HPG trapped within fixed cells. C2C12 cells were labelled with (i-v) or without (vi) HPG. For i-v inhibitors of translation were also included: cycloheximide (i), Harringtonine (ii), Pactamycin (iii), Puromycin (iv) or cycloheximide plus chloramphenicol (v). All click images were visualised for 5 seconds and displayed with the same brightness and contrast settings. Scale bar: 20 µm.

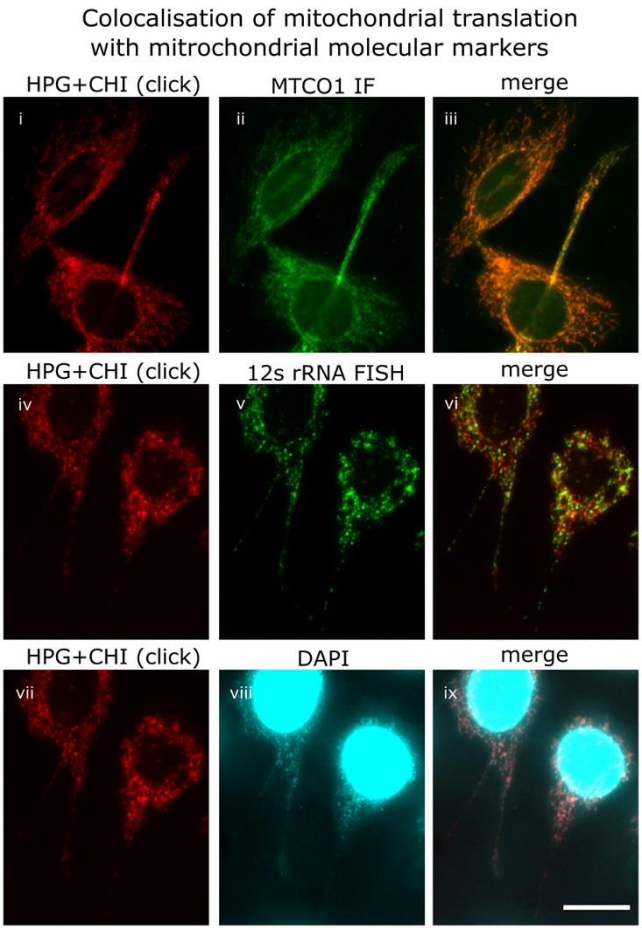

Figure 4: Colocalisation of CHI-resistant HPG incorporation with MT-CO1, 12s rRNA and cytoplasmic DNA. C2C12 cells were labelled with HPG in the presence of cycloheximide and translation detected by click reaction with fluorescent azide (i,iv, vii). Subsequently MT-CO1 protein was detected by immunofluorescence (ii), 12s rRNA was detected by RNA FISH (v) and DNA by DAPI staining (viii). DAPI exposure was for 500 ms, ~ fifty times longer than normally used for nuclear DNA imaging. Merged images show colocalisation of these three molecular markers with mitochondrial translation (iii, vi, ix)). Co-localisation of MT-CO1 and Mt translation was quantified using Image J with the COL2 plugin on 18 cells giving a Pearson's mean co-localization coefficient of 0.90 (i.e. 90% Co-localisation), +/- SD = 0.04. Scale bar: 20 µm.

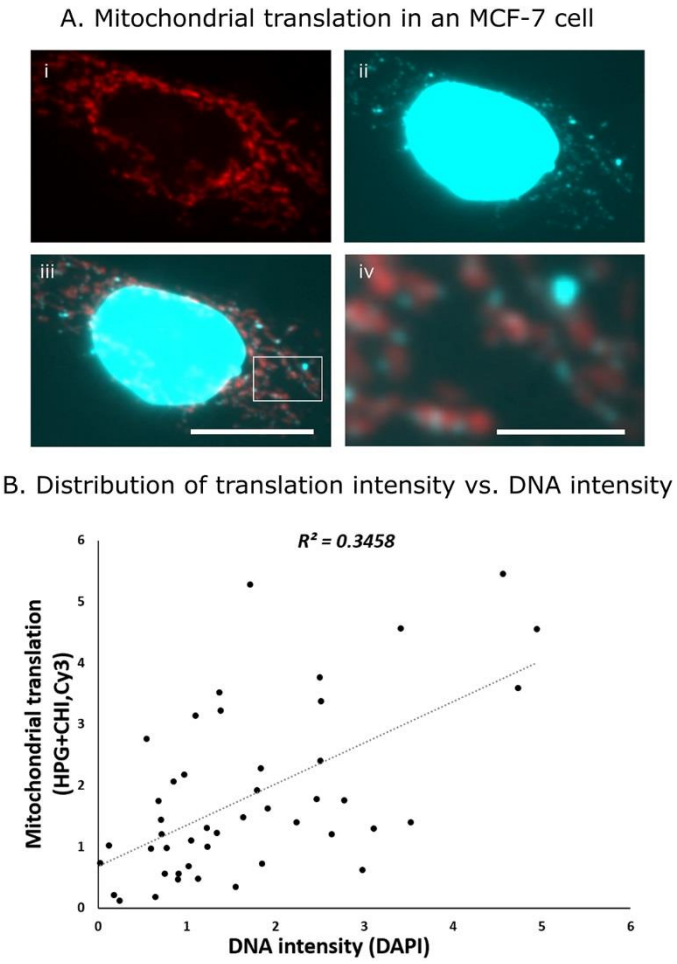

Figure 5: Strength of mitochondrial translation does not correlate perfectly with amount of mitochondrial DNA.

A. MCF-7 cells were labelled with HPG in the presence of cycloheximide, mitochondrial translation was detected by click reaction with a fluorescent azide (i). Staining with DAPI and prolonged camera exposure allowed imaging of mitochondrial DNA as punctate spots and rods in the cytoplasm (ii). The merged image and magnified inset (iii, iv) show the blue DAPI staining signal lying within or adjacent to the products of mitochondrial translation. Scale bar: 20 µm (i-iii), 5 µm (iv). B. 46 ROIs in total from 7 cells were created using ImageJ. Each ROI encompassed punctate cytoplasmic DAPI staining and surrounding fluorescence from adjacent mitochondrial translation. Mean Red (translation) and blue (DNA) fluorescence was calculated for each ROI. Background fluorescence in both channels was calculated from each cell individually as the mean of at least 4 ROIs that lacked either punctate DAPI staining or rod-like red fluorescence and subtracted from values obtained from each mitochondrial region within that cell. These total corrected red and blue florescence values for each region were plotted and a regression line and R^2 value calculated using Microsoft Excel software.

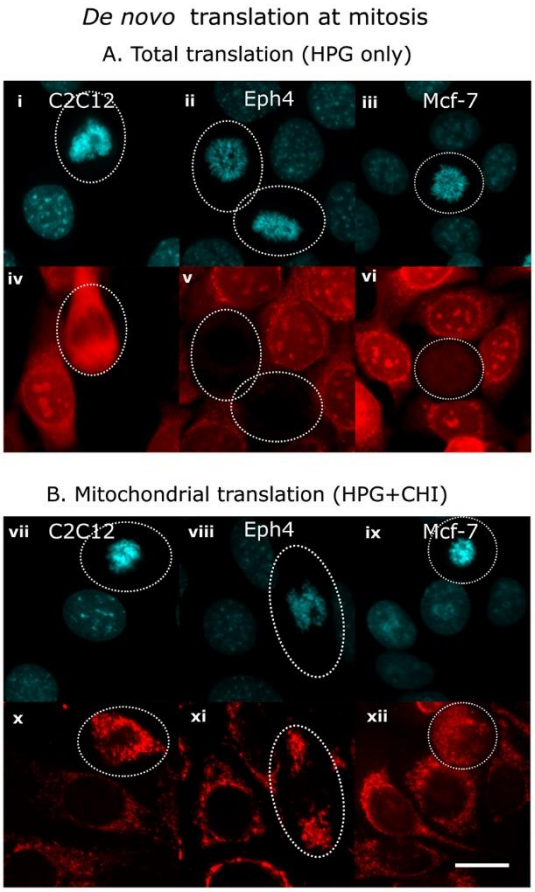

Figure 6: *De novo* translation at mitosis. C2C12, Eph4 and MCF-7 cells were labelled with HPG without (A) or with (B) cycloheximide, DAPI stained ((i-iii; vii-ix) and newly translated proteins detected by click reaction with a fluorescent azide (iv-vii; x-xii). Mitotic cells at prometaphase are encircled. Scale bar: 20 µm

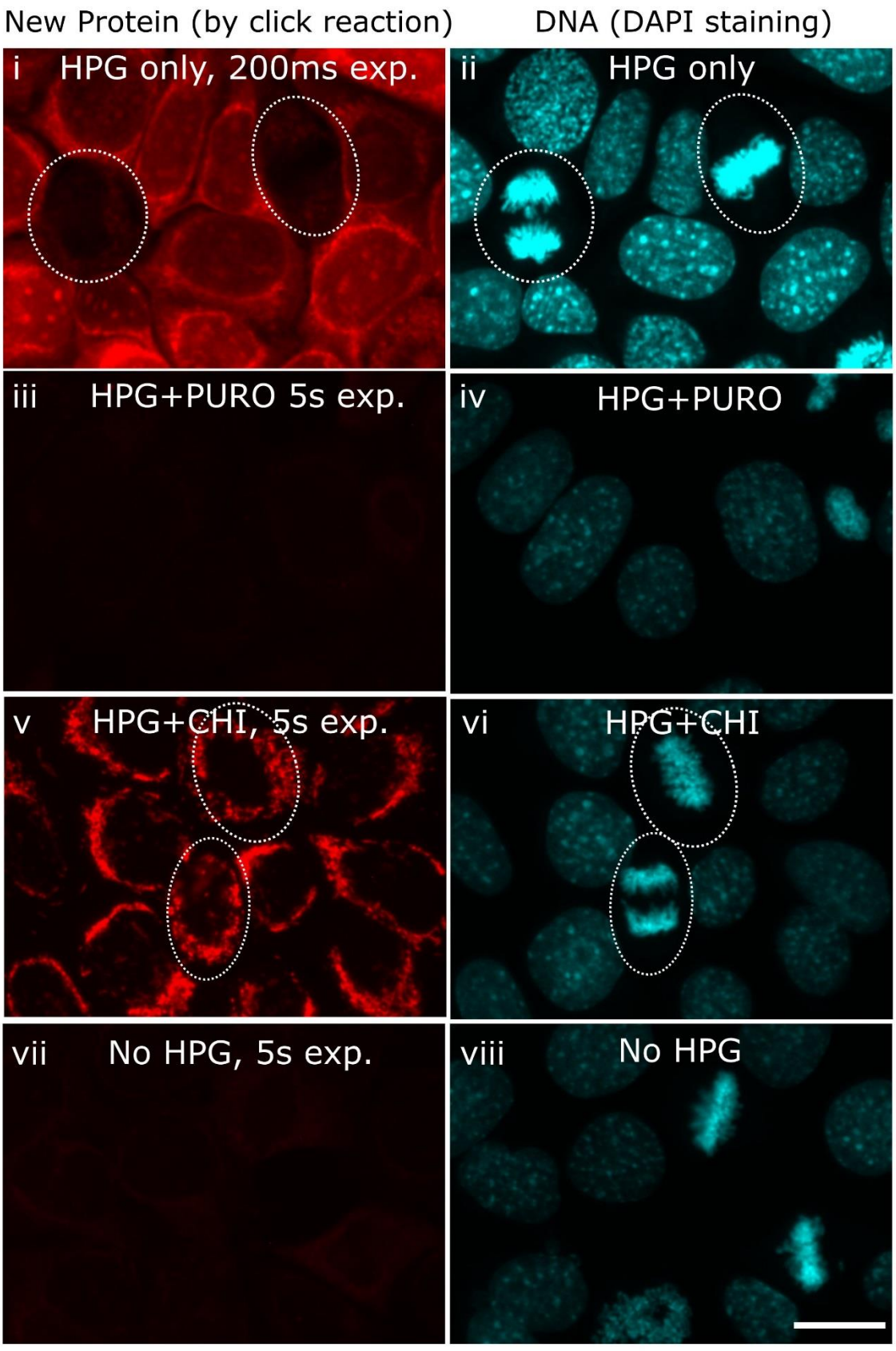

Supplementary Figure 1 Protein synthesis in Eph4 cells with or without cycloheximide. Eph4 cells were labelled with HPG in the presence or absence of cycloheximide and alkyne-labelled proteins detected by epifluorescence microscopy after a “click” reaction on fixed cells with a fluorescent azide. 200 ms exposures of cells treated with HPG (i,ii); 5 s exposures of cells treated with HPG and puromycin (iii,iv); 5 s exposures of cells treated with HPG and cycloheximide (v,vi); 5 s exposures of cells without HPG (vii, viii). Images with same exposure times displayed with identical brightness and contrast settings; mitotic cells in i,ii,v and vi are encircled by dashed lines. Scale bar: 20 µm.

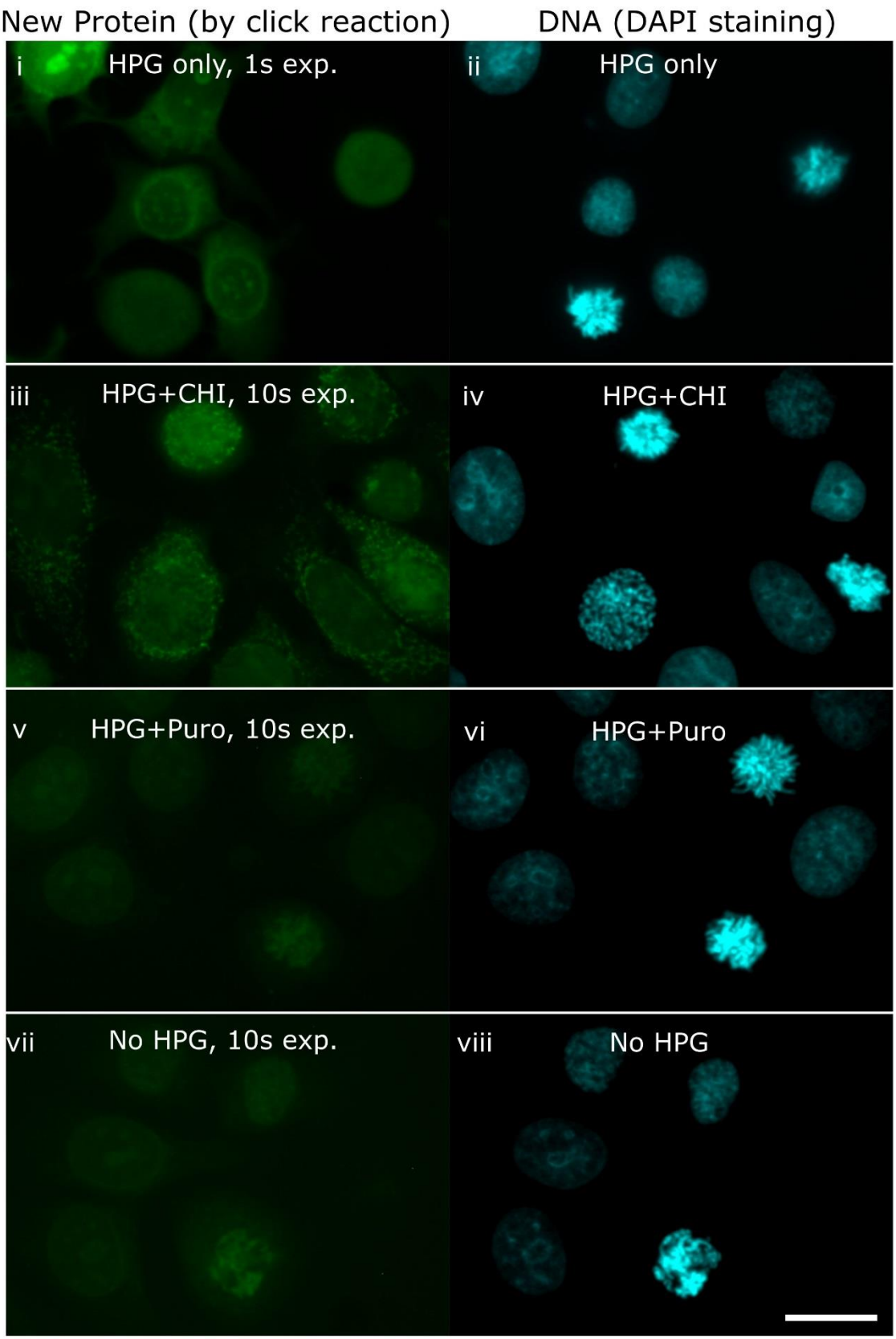

Supplementary Figure 2 Protein synthesis in MCF-7 cells.. MCF-7 cells were labelled with HPG (i, ii), HPG+cycloheximide (iii,iv), HPG + puromycin (v,vi) or without HPG (vii, viii) and alkyne-labelled proteins detected by epifluorescence microscopy after a “click” reaction on fixed cells with a fluorescent azide. Exposure times for click imaging were 1 s (i) or 10 s (iii, v, vii). Images with same exposure times displayed with identical brightness and contrast settings scale bar: 20 µm.

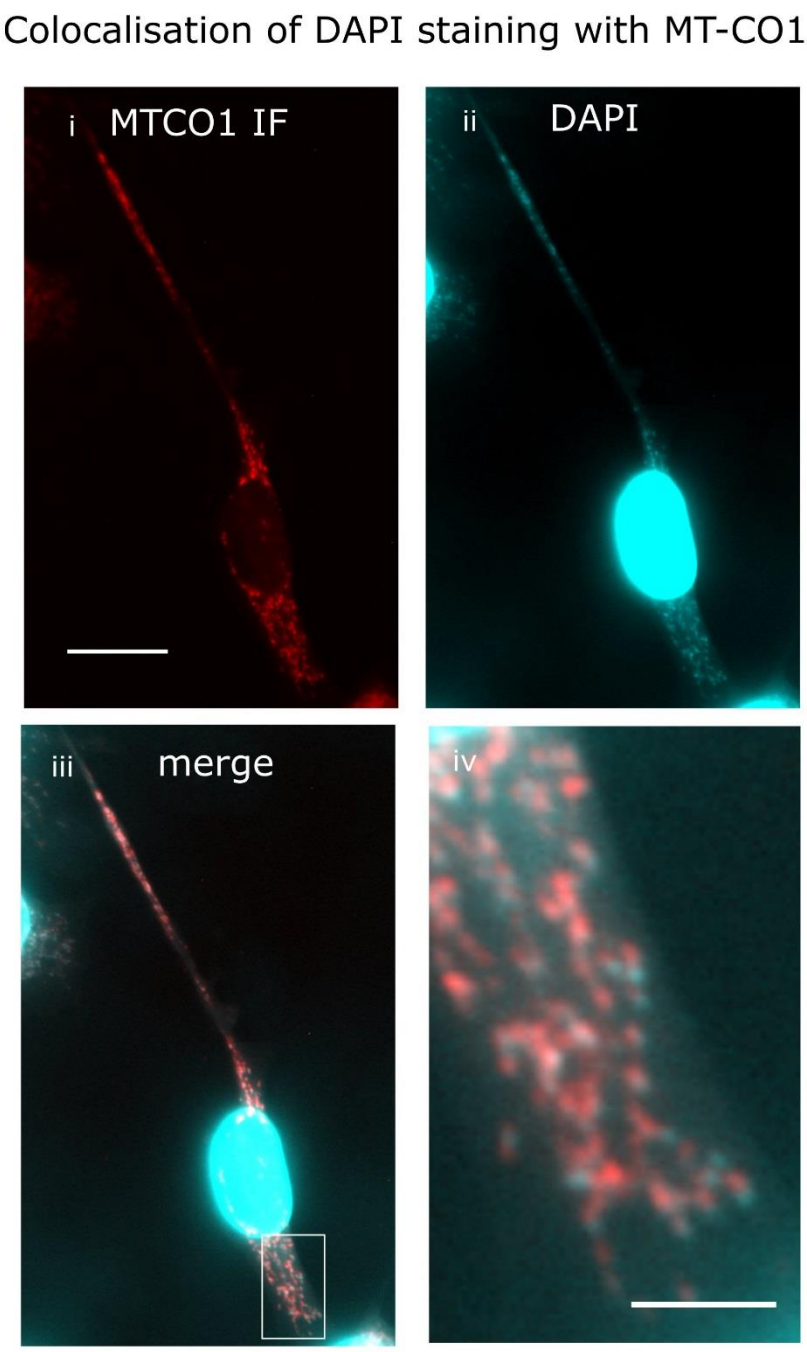

Supplementary Figure 3: Co-localisation of MT-CO1 cytoplasmic DNA in C2C12 cells. MT-CO1 protein was detected by immunofluorescence (i), DNA by DAPI staining (ii). DAPI exposure was for 1 s. Merged images (iii,iv) show co-localisation. Scale bars are 20 µm (i-iii) and 5 µm (iv).